

## Brainstem glucose hypermetabolism in ALS/FTD and shorten survival: a $^{18}\text{F}$ -FDG PET/MR study

Matteo Zanovello<sup>1</sup>, Gianni Sorarù<sup>1,2</sup>, Cristina Campi<sup>3</sup>, Mariagiulia Anglani<sup>4</sup>, Alessandro Spimpolo<sup>5</sup>, Sara Berti<sup>5</sup>, Cinzia Bussè<sup>1</sup>, Stefano Mozzetta<sup>1</sup>, Annachiara Cagnin<sup>1,2</sup>, Diego Cecchin<sup>2,5</sup>

### Affiliations:

<sup>1</sup>Neurology Unit, Department of Neurosciences (DNS), University of Padova, Italy

<sup>2</sup>Padova Neuroscience Center, University of Padova, Padova, Italy

<sup>3</sup>Mathematics, Department of Mathematics, University of Genova, Genova, Italy.

<sup>4</sup>Neuroradiology Unit, Department of Neurology, University-Hospital of Padova, Italy

<sup>5</sup>Nuclear Medicine Unit, Department of Medicine (DIMED), University-Hospital of Padova, Italy

### Corresponding author:

Prof. Diego Cecchin, MD

Department of Medicine (DIMED)

University-Hospital of Padova

Via Giustiniani 2, 35128 Padova, Italy

Tel.: +39 49 8213020

Email: [diego.cecchin@unipd.it](mailto:diego.cecchin@unipd.it)

### Disclosures:

- Matteo Zanovello: nothing to disclose
- Gianni Sorarù: nothing to disclose
- Cristina Campi: nothing to disclose
- Mariagiulia Anglani: nothing to disclose
- Alessandro Spimpolo: nothing to disclose
- Sara Berti: nothing to disclose
- Cinzia Bussè: nothing to disclose
- Stefano Mozzetta: nothing to disclose
- Annachiara Cagnin: nothing to disclose
- Diego Cecchin: nothing to disclose

Keywords: Amyotrophic Lateral Sclerosis, FTD, PET, survival, brainstem

## **Abstract**

### **Introduction:**

A few  $^{18}\text{F}$ -FDG (FDG) PET-CT studies revealed the presence of brain hypermetabolism in the brainstem and cervical spinal cord of patients within the Amyotrophic Lateral Sclerosis continuum (ALS/FTD). We aim to investigate this finding through a hybrid PET-MR system, allowing a more precise spatial pattern of metabolic changes in the brainstem and cervical spinal cord.

### **Method:**

Twenty-eight patients with a diagnosis of ALS or behavioural variant FTD plus motoneuron disease and thirteen control subjects underwent  $^{18}\text{F}$ -FDG PET-MR study. Mean normalized FDG uptake values in the midbrain/pons, medulla oblongata, and cervical spinal cord defined on individual's MR scans were compared between groups. Furthermore, the associations between regional FDG uptake values and clinical and demographic characteristics, including gene mutation, type of onset (bulbar, spinal, dementia), and clinical characteristics were investigated.

### **Results:**

A significant ( $p < 0.005$ ) increment in glucose metabolism in the midbrain/pons and medulla oblongata was found in ALS/FTD patients (spinal-ALS and FTD-MND subgroups) in comparison to controls. No relevant associations between clinical and metabolic features were reported, although medulla oblongata hypermetabolism was associated with shortened survival ( $p < 0.001$ ).

### **Conclusion:**

Increased glucose metabolism in the brainstem might be due to neuroinflammation, one of the key steps in the pathogenic cascade that leads to neurodegeneration in ALS/FTD. FDG PET-MR could be a valuable tool to assess glial changes in the ALS/FTD spectrum and could serve as a prognostic biomarker. Large prospective initiatives would likely shed more light on the promising application of PET-MR in this setting.

## Introduction

The clinical overlap between amyotrophic lateral sclerosis (ALS) and frontotemporal dementia (FTD) has been widely recognised, with behavioural/cognitive symptoms occurring in a certain amount of patients with ALS, and signs of motoneuron disease in a number of FTD.<sup>1</sup> This, along with the discoveries of shared genetics and pathophysiological mechanisms, has informed the recharacterization of the two diseases as the extremes of a common neurodegenerative spectrum (ALS/FTD).

From a pathophysiologic perspective, these diseases present proteinaceous cytoplasmic aggregates that eventually lead to neuronal degeneration and loss. Glial cells are also actively involved in the ALS/FTD pathology. Amongst these are astrocytes, which causes excitotoxicity when their role in synaptic glutamate reuptake is impaired, and microglia, which phenotype evolves from neuroprotective to neurotoxic through the course of the disease.<sup>2</sup> Neuropathological studies in ALS patients have found depletion of motor neurons and diffuse glial infiltration in the grey and white matter of the spinal cord and the motor cortex.<sup>3</sup> As predicted, both activated microglia and astrocyte markers have been observed in imaging studies of ALS<sup>4,5</sup> and FTD patients.<sup>6,7</sup>

Several neuroimaging techniques have been applied to ALS and FTD cohorts to explore their use as potential disease biomarkers. Cortical MR hallmarks of ALS are bilateral atrophy of the primary motor cortex (precentral gyrus), and degeneration of the corticospinal tract and corpus callosum.<sup>8</sup> A MR study including diffusion tensor imaging<sup>9</sup> showed reduced fractional anisotropy in corticospinal tracts, frontal and temporal lobes, and in the regions that connect the motor and premotor cortex. Moreover, at a functional level, changes of connectivity of neural networks within motor and extra-motor domains have been demonstrated through EEG<sup>10</sup> and fMRI<sup>11</sup> studies. These insights, in line with findings that show how patients with different degrees of cognitive impairment have significantly different patterns of frontal lobe metabolic impairment when assessed using 18-2-Fluoro-2-Deoxy-D-Glucose (<sup>18</sup>F-FDG) PET,<sup>12</sup> could partially explain the heterogeneous clinical manifestations and spreading of the disease.

In line with this, several PET-CT studies in ALS/FTD patients, including proven C9orf72 carriers, focused on cortical structures, showing frontal and temporal hypometabolism.<sup>13,14</sup> Conversely, the few that explored other CNS regions found

increased  $^{18}\text{F}$ -FDG uptake in the cerebellum, brainstem,<sup>15,16</sup> and spinal cord<sup>17,18,19</sup> of patients with ALS when compared to controls. The reason for the increase in the regional glucose uptake is still a matter of debate.

In light of these findings, we chose to assess glucose metabolic patterns analysing separately midbrain/pons, medulla oblongata, and cervical spinal cord of ALS/FTD patients, as compared to control subjects, by means of co-acquired PET and MR images. As PET-CT images can lead to difficulties in delineating VOIs, this is the first study in this setting to exploit the potential of the hybrid PET-MR technique which, relating  $^{18}\text{F}$ -FDG values to precise anatomical substrates, can improve result accuracy. Furthermore, we aimed to estimate the association between the degree of FDG-uptake and clinical characteristics such as type of clinical presentation, including the site of onset, presence of the C9orf72 mutation, disease progression, and survival.

## **Materials and Methods**

### **Participants**

A total of 28 patients diagnosed with ALS (n=16) or FTD who developed plus motor neuron disease in the course of the disease (n=12), who underwent <sup>18</sup>F-FDG PET-MR (Biograph mMR; Siemens, Erlangen, Germany) at the Nuclear Medicine Unit of the University of Padova, were retrospectively recruited between July and December 2019. Probable or definite ALS was diagnosed according to El Escorial revised criteria<sup>20</sup> and the diagnosis was confirmed in all patients during their clinical follow-up. Patients with FTD were diagnosed with a behavioural variant FTD (bvFTD) according to Raskosky criteria<sup>21</sup> and developed signs of motor neuron disease. The median time between diagnosis and <sup>18</sup>F-FDG PET-MR scan was 1 month.

Thirteen participants, who were referred to the Nuclear Medicine Unit with a diagnosis other than neurological diseases and were not showing any signs of brain disease under the same scanning procedure, served as control subjects (CS).

The 28 patients were further classified according to the clinical presentation at the time of diagnosis as bulbar ALS (N=5) and spinal ALS (N=11) or FTD-MND patients (N=12). Six patients (2 with spinal ALS and 4 with FTD-MND) carried a GGGGCC hexanucleotide repeat expansion in the first intron of the C9orf72 gene and one (spinal ALS) carried a mutation of the *VCP* gene (9p13.3) coding for the Valosin Containing Protein.

The exclusion criteria included having a history of other neurological disorders, cerebrovascular disease, diabetes mellitus or systemic inflammatory disease. Moreover, other exclusion criteria were diagnostic uncertainty according to the El Escorial revised criteria, and PET-MR scans non-evaluable due to significant movement artefacts. The local ethical committee approved the retrospective study (protocol number: AOP1673 - 4831/AO/20). All patients and controls gave written informed consent before undergoing the <sup>18</sup>F-FDG PET-MR in accordance with the principles outlined in the Declaration of Helsinki.

### **Clinical data**

Demographic variables, as well as the time elapsed from onset or diagnosis to <sup>18</sup>F-FDG PET/MR scan, were obtained for each patient. Moreover, the ALS-Functional Rating Scale revised (ALS-FRS-r) was calculated (for ALS patients only, being a retrospective

study) both at the time of diagnosis and at the latest available neurologic visit. ~~and scan,~~  
~~whereas.~~ Furthermore a progression rate, also known as  $\Delta$ -ALS-FRS-r,<sup>22</sup> was calculated as  $\Delta$ FS=(48 - ALSFRS-r at “time of diagnosis”)/duration from onset to diagnosis (month) for 15/18 ALS patients (for 3 patients ALSFRS-R was not available at the time of diagnosis). Muscle strength was assessed through the Medical Research Council (MRC) scale.

### **Image acquisition and analysis**

PET-MR were acquired between July 2015 and November 2019 and, following the European Association of Nuclear Medicine (EANM) guidelines,<sup>23</sup> patients had to fast for 6 hours before the injection of the radiopharmaceutical, and blood glucose was assessed to be less than 200 mg/dl; a single i.v. bolus of 3 MBq/kg <sup>18</sup>F-FDG was injected in resting conditions (in a dim light room with closed eyes) prior to the scan. PET and MR scans were simultaneously acquired using a Siemens Healthcare Biograph mMR, which included several sequences (T1, T2-weighted, SWI, and DWI) and a PET brain scan (acquisition time 1500 sec. reconstructed using a 344x344 mm matrix and a 3D iterative reconstruction algorithm).

Postprocessing was carried out using the “Image Fusion” tool within PMOD software (PMOD Technologies LLC, Zurich, Switzerland): briefly, each <sup>18</sup>F-FDG-PET scan was finely realigned to the pertinent 3D, isotropic (1mm) T1-weighted MR scan based on a rigid transformation (smoothing: Gaussian filter width 6.0 mm; dissimilarity function: normalized mutual information; interpolation method: trilinear; sample rate: 5.2/4.0 mm start/final; minimization method: Powell; function tolerance: 1.0-4).

PMOD was then used to create VOIs (Volumes of Interest, Figure 1) both for patients and CS as follows:

- Manual positioning, on 3D T1w images, of visually adjusted cubical VOIs respectively on midbrain/pons, medulla oblongata, cervical spinal cord (the region between skull basis and the plane adjacent to the caudal face of C4 vertebral body)
- Isocounting (inside the defined cubical VOIs) with a threshold higher than 40% of the overall maximum uptake, several 3D VOIs were outlined (midbrain/pons, medulla oblongata, and cervical spinal cord).
- Manual positioning of visually adjusted spherical VOIs in the parieto-occipital white matter (as background VOIs) on the T1-weighted MR.

For each subject, the mean uptake within each volume of interest was normalized using the mean uptake of the occipital white matter background VOIs<sup>24</sup> as the area is reported to experience fewer <sup>18</sup>F-FDG metabolic alterations in previous works<sup>14</sup>.

### **Statistical analysis**

All data are reported as means  $\pm$  standard deviation (SD). After evaluating the gaussian distribution of data, unpaired t-tests were performed to relate uptake value to categorical variables, whereas continuous variables were analysed through correlation and linear regression testing. Since patient and control age distribution was found to be significantly different, residual analysis for regression was applied when comparing the two groups<sup>25</sup>. Log-rank test was applied for survival analysis. A p-value  $< 0.05$  was considered significant. Univariate and multivariate survival analysis (considering genetics, site of onset, age at PET and time from onset to PET) have been performed.

## Results

The main clinical findings in ALS/FTD patients and control subjects are shown in Table 1 and 2. No significant differences were found between the sex, weight, and height of the two groups, whereas the age distribution between patients ( $62.6 \pm 8.2$  years) and controls ( $52.8 \pm 13.6$  years) differed significantly.

Examining MR T2-Flair sequence we found mild to moderate cortico-spinal tract hyperintensities in 8% of FTD-MND patients and 40% of ALS subjects. SWI (available only for ALS patients) revealed variable degree of motor band sign (cortical ferromagnetic deposition in primary motor cortex) in 64% of subjects.

We examined the relationship between metabolic patterns within the VOIs under examination with other clinical measures and the genetic background (C9orf72 mutation), although none of them showed a significant association.

After the PET-MR study follow-up lasted between 2 and 55 months (median 33 months), during which patients showed a steep drop in their average ALS-FRS-r score (from  $37.2 \pm 6.5$  to  $29.4 \pm 10.6$ ). The calculated progression rate (Table 2) mildly correlates with medulla oblongata hypermetabolism (correlation coefficient: 0.45) but not with pontine (correlation coefficient: -0.02) or cervical spinal cord (correlation coefficient: 0.3) hypermetabolism. The variation of ALS-FRS-r score (last ALS-FRS-r as compared to first one) demonstrated however no significant correlation with FDG hypermetabolism considering pontine (correlation coefficient: -0.13), medulla oblongata (correlation coefficient: 0.31), or cervical spinal cord (correlation coefficient: 0.31) regions.

During the study follow-up, 10 (7 ALS and 3 FTD-MND) patients died; however, univariate Cox regression analysis did not prove significant for C9orf72 mutation, sex, clinical phenotype, or cognitive impairment (FTD-MND patients).

An analysis of the metabolic patterns of midbrain/pons, medulla oblongata, and cervical spinal cord revealed a strong correlation between metabolic patterns of the three VOIs (Figure 2A). Moreover, as visible from the density plots (Figure 2B), the distribution of the uptake values was unbalanced between controls and patients, the former showing less  $^{18}\text{F}$ -FDG uptake in all the regions under examination compared to the latter.

After normalization for the background VOIs and adjustment for age<sup>25</sup>, an increase in glucose metabolism in ALS/FTD patients, when compared to controls, was detected in all

the three regions under examination. FDG uptake reached significant higher values for patients compared to controls in midbrain/pons and medulla oblongata (Figure 3), but not in the cervical spinal cord.

Analysis of spinal, bulbar, and FTD-MND subgroups showed a statistically significant relative hypermetabolism in the midbrain/pons and medulla oblongata when normalized to the white matter in patients with spinal and behavioural onset with respect to controls (Figure 4). Uptake values in patients with bulbar onset were not significantly different from controls, most likely because of their small numerosity (n=5). On the other hand, analysis between the three subgroups (bulbar, spinal, and FTD-MND) did not show any significant difference in <sup>18</sup>F-FDG uptake values in any of the explored regions, apart from the cervical spinal cord between spinal and bulbar onset patients.

The Kaplan-Meier analysis and univariate Cox regression analysis (Table 3) at 50 months after PET/MR showed that the patients with normalized medulla oblongata uptake above the fifth decile (9/16 ALS and 5/12 FTD-MND presented normalized medulla oblongata uptake > 50%) had a significantly higher mortality rate than those below the fifth decile (log-rank test,  $p < 0.001$ ) (Figure 5), whereas the analysis results were not significant for the other regions under examination. A multivariate Cox regression analysis confirmed that an higher medulla oblongata uptake and a longer “time from symptoms onset to PET” are independently associated with a shorter survival (Table 3). Clinical bulbar signs (such as dysarthria and dysphagia), at the time of PET examination (in 9/16 ALS and 2/12 FTD-MND subjects) were not statistically correlated (corr. coefficient:0.18) with normalized hypermetabolism in medulla oblongata

## Discussion and Conclusions

This study, to our current knowledge, is the first to exploit an integrated  $^{18}\text{F}$ -FDG-PET-MR to study the metabolic patterns of patients with ALS and FTD. In our population MR could be useful when differentiating ALS subjects from FTD-MND because cortico-spinal tract hyperintensities seem to be more frequent in the former group (40% vs 8%). Furthermore we have noticed motor band sign (SWI sequence) in the majority (64%) of ALS subjects. This qualitative finding could complement, at a single subject level, the diagnostic accuracy of PET regional glucose hyper and hypometabolism.

We detected midbrain/pons and medulla oblongata increased uptake values in patients as compared to controls, confirming previous PET-CT findings.<sup>15,16</sup> Furthermore, we described how medulla oblongata metabolism relates to patient survival, suggesting a possible prognostic value for PET-MR.

Results of our study indicated that the uptake of all three brain regions investigated (midbrain/pons, medulla oblongata, cervical spinal cord) are significantly correlated, as shown by the paired correlation (Figure 2A). An explanation for the correlation of metabolic patterns in the three regions is the involvement of the corticospinal and corticobulbar tracts containing the projections of upper motor neurons from the motor cortex. A bimodal distribution could be seen in the density plot distribution of controls as compared to the “ALS/FTD continuum” in Fig. 2B. The second lower peak of the bimodal distribution is however due to a single, slightly outlier, control subject.

Theoretically, the expected effect of a neurodegenerative disease is a reduction in tissue metabolic rate caused by neuronal loss; indeed, frontal hypometabolism is one of the cortical signatures of the diseases along the ALS/FTD spectrum.<sup>12,13,14</sup> Nevertheless, strong evidence has been brought in favour of neuroinflammation as one of the key steps in the pathogenic cascade that leads to ALS/FTD. Initially described in pathology studies, glial infiltration has later been confirmed in vivo both in models and humans.<sup>4,5</sup>

A possible explanation, which links neuroinflammation with neurodegeneration, involves these two types of glial cells, namely activated microglia and astrocytes. Activated microglia, which has been found in the motor cortex, pons, and thalamus of patients with ALS, contributes to the pathogenesis propagating and sustaining the tissue damage through the release of free radicals and other neurotoxic substances such as glutamate.

Moreover, a shift from a neuroprotective (M2) to a disrupting (M1) phenotype is apparent since the early stages of the disease.<sup>2</sup> Astrocytes physiologically account for a consistent share of CNS glucose consumption. Thereafter, they start glycolysis to provide lactate to neurons; in hindsight, astrocytes play a key role in coupling glucose metabolism with synaptic activity. In the case of neurodegeneration, glutamate excess leads to an increased glucose accumulation in astrocytes, even though neurons degenerate.<sup>26</sup> Moreover, during the course of the disease, astrocytes replace dead neurons and axons following the corticospinal and corticobulbar tracts, furtherly increasing the metabolic uptake of the degenerating brain region. Neuroimaging evidence for the involvement of these glial cells in the pathogenesis of ALS/FTD has been brought by studies that exploited neuroinflammation-specific ligands, including <sup>11</sup>C-L-deprenyl-D2,<sup>4</sup> mapping astrocyte activation, the activated microglia marker <sup>11</sup>C(R)-PK11195,<sup>5,6</sup> and TSPO-ligand <sup>18</sup>F-DPA-714<sup>27</sup>, showing increased tracer uptake along the corticospinal tract.

From a metabolic perspective, these phenomena result in an increased relative <sup>18</sup>F-FDG uptake in regions of neuronal degeneration in affected individuals compared to control. However, when evaluating the relative weight of the two cells types, it must be considered that the microglia seems to relate more with hypometabolic areas, as shown in frontotemporal areas of FTD patients,<sup>5,6</sup> whereas astrocytosis drives glucose consumption and it is, therefore, more likely associated with the hypermetabolic burden,<sup>26</sup> in line with previous findings.<sup>4</sup> We acknowledge that this evidence cannot prove the exclusive role of one of these two glial cells, which is based on a continuous interplay involving also other cell types, and that longitudinal studies will be needed to better characterize the interplay between neurodegeneration and hypermetabolism, and its different behaviour in upper and lower motor neurons.

An alternative reason for the finding of glucose hypermetabolism in ALS/FTD patients can be related to a methodological issue involving the normalization process of FDG data. We normalized the uptake values of the regions of interest for the values of the occipital white matter to exclude interindividual differences. On the contrary, normalizing for other regions would require an a priori assumption, namely that none of the background VOIs shall be affected by hypo- or hypermetabolism. In the present study occipital white matter has been chosen as the reference because it seems spared from the ALS/FTD

neurodegenerative process,<sup>14,24</sup> and none of the PET-CT studies on subjects affected with the disease showed significant metabolic variations in that region.

Another issue we faced was the different age distribution between the two groups. To ignore this effect on the uptake values, we adjusted for age through a linear regression model<sup>25</sup> and we then used the residual values for the group analysis (Figure 3). It is to be noted, however, that we usually expect a higher metabolism in younger patients with respect to controls. On the contrary, in this setting, although controls are younger than patients, they present a lower metabolism; this fact reassures us of the choice of groups selected and of the obtained results.

Although considering a small cohort, the subgroup analysis included patients with different ALS onset, namely spinal (n=11), bulbar (n=5), and behavioural/cognitive (n=12). While spinal or behavioural onset groups showed higher FDG uptake with respect to controls, bulbar onset did not prove significant because of the small number of individuals in the latter group. Interestingly, density plot of normalized FDG uptake in FTD-MND was similar to that of patients with ALS (Figure 2,4). Therefore, we can state that hypermetabolism in the corticospinal tract could be a common feature for all the ALS subgroups, thereby suggesting, once again, common metabolic and pathophysiologic patterns within the disease spectrum. Prospective studies involving a larger number of individuals with different sites of onset, including FTD patients without clinical MND, as well as comparisons between cortical and subcortical regions with lower motor neurons (to elucidate the possible metabolic relations between upper and lower motor neurons), are expected to increase current results.

Bulbar onset ALS is a prognostic factor associated with short survival.<sup>28</sup> Here, we instead showed how the metabolic uptake of medulla oblongata was significantly associated with short survival (Figure 5). This finding supports the hypothesis for which neuroinflammation of midbrain structures is one of the main mechanisms involved in ALS progression and highlights a potential role for neurometabolic studies as prognostic and outcome predictors. Moreover, a previous study<sup>17</sup> reported a significant relationship between the whole spinal cord normalized uptake value and patient survival, thus it will be necessary to compare the metabolic patterns of these two regions to draw consistent evidence.

In conclusion, this study is the first to analyse the brain metabolism of ALS/FTD patients through the hybrid PET-MR technique and to demonstrate that bulbar uptake could be a strong survival predictor.

Notwithstanding the limited sample size and the retrospective design, we confirmed the presence of increased glucose metabolism in the midbrain/pons and medulla oblongata, supporting the importance of neuroinflammation in the disease spectrum pathogenesis. Considering the present need for reliable diagnostic and prognostic biomarkers in ALS and FTD, our results support PET neuroimaging as one of the most promising candidates for this role, although the cost and expertise required pose a barrier to the translation of this technology to clinical practice. A further step will be to design longitudinal studies involving large cohorts of age-matched patients, individuals with ALS-mimics and healthy controls, to assess early predictive values of PET imaging, understand the neuroradiologic course of the disease, and evaluate the effect of therapies. These studies will need to thoroughly indagate CNS metabolism and to relate metabolic patterns within different brain regions to disease genotype and phenotype, with particular regard to the differences between upper and lower motor neuron involvement.

**Compliance with Ethical Standards:**

**Funding:** This research received no external funding.

**Disclosure of potential conflicts of interest:** All the authors declare no conflict of interest.

**Research involving human participants and/or animals:** All procedures performed in studies involving human participants were in accordance with the ethical standards of the institutional and/or national research committee and with the 1964 Helsinki declaration and its later amendments or comparable ethical standards. This was a single-center, retrospective, observational study conducted after formal approval by our local Ethics Committee (protocol number: AOP1673 - 4831/AO/20).

**Informed consent:** All patients gave written informed consent before undergoing the PET-MR scan

**Author Contributions:** Conceptualization, M.Z., G.S., A.C. and D.C.; methodology, C.C., S.B., C.B., A.S. and D.C.; software, M.Z. and C.C.; formal analysis, S.M.; C.C.; data curation, S.M., M.A., C.C. and D.C.; writing—original draft preparation, M.Z., A.C. and D.C.; writing—review and editing, G.S., M.A., A.S., C.B., A.C., and D.C.; project administration, D.C. All authors read and agreed to the published version of the manuscript.

**KEY POINTS:**

**QUESTION:** Is there a significant increment in glucose metabolism in the midbrain/pons and medulla oblongata of ALS/FTD patients as compared to controls ? And is it related to mortality rates ?

**PERTINENT FINDINGS:**

An increase in glucose metabolism in ALS/FTD patients, as compared to controls, was noted in all the three regions under examination (midbrain/pons, medulla oblongata, cervical spinal cord). The Kaplan-Meier analysis at 50 months after PET/MR showed that the patients with normalized medulla oblongata uptake above the fifth decile had a significantly higher mortality rate than those below the fifth decile (log-rank test,  $p < 0.001$ )

**IMPLICATIONS FOR PATIENT CARE:**

Considering the present need for reliable diagnostic and prognostic biomarkers in ALS and FTD, our results support PET neuroimaging of medulla oblongata as one of the most promising candidates for this role

## REFERENCES:

1. Robberecht W, Philips T. The changing scene of amyotrophic lateral sclerosis. *Nat Rev Neurosci*. 2013;14:248-64.
2. McCauley ME, Baloh RH. Inflammation in ALS/FTD pathogenesis. *Acta Neuropathol*. 2019;137:715-730.
3. Ince PG, Highley JR, Kirby J, et al. Molecular pathology and genetic advances in amyotrophic lateral sclerosis: an emerging molecular pathway and the significance of glial pathology. *Acta Neuropathol*. 2011;122:657-71.
4. Johansson A, Engler H, Blomquist G, et al. Evidence for astrocytosis in ALS demonstrated by [11C](L)-deprenyl-D2 PET. *J Neurol Sci*. 2007;255:17-22.
5. Turner MR, Cagnin A, Turkheimer FE, et al. Evidence of widespread cerebral microglial activation in amyotrophic lateral sclerosis: an [11C](R)-PK11195 positron emission tomography study. *Neurobiol Dis*. 2004;15:601-9.
6. Bevan-Jones WR, Cope TE, Jones PS, et al. Neuroinflammation and protein aggregation co-localize across the frontotemporal dementia spectrum. *Brain*. 2020;143:1010-1026.
7. Cagnin A, Rossor M, Sampson EL, Mackinnon T, Banati RB. In vivo detection of microglial activation in frontotemporal dementia. *Ann Neurol*. 2004;56:894-7.
8. Agosta F, Valsasina P, Riva N, et al. The cortical signature of amyotrophic lateral sclerosis. *PLoS One*. 2012;7:e42816.
9. Crespi C, Dodich A, Cappa SF, et al. Multimodal MRI quantification of the common neurostructural bases within the FTD-ALS continuum. *Neurobiol Aging*. 2018;62:95-104.
10. Iyer PM, Egan C, Pinto-Grau M, et al. Functional Connectivity Changes in Resting-State EEG as Potential Biomarker for Amyotrophic Lateral Sclerosis. *PLoS One*. 2015;10:e0128682.
11. Trojsi F, Esposito F, de Stefano M, et al. Functional overlap and divergence between ALS and bvFTD. *Neurobiol Aging*. 2015;36:413-23.
12. Canosa A, Pagani M, Cistaro A, et al. 18F-FDG-PET correlates of cognitive impairment in ALS. *Neurology*. 2016;86:44-9.
13. Cistaro A, Pagani M, Montuschi A, et al. The metabolic signature of C9ORF72-related ALS: FDG PET comparison with nonmutated patients. *Eur J Nucl Med Mol Imaging*. 2014;41:844-52.
14. Chiò A, Pagani M, Agosta F, Calvo A, Cistaro A, Filippi M. Neuroimaging in amyotrophic lateral sclerosis: insights into structural and functional changes. *Lancet Neurol*. 2014;13:1228-40.
15. Van Laere K, Vanhee A, Verschueren J, et al. Value of 18fluorodeoxyglucose-positron-emission tomography in amyotrophic lateral sclerosis: a prospective study. *JAMA Neurol*. 2014;71:553-61.
16. Pagani M, Chiò A, Valentini MC, et al. Functional pattern of brain FDG-PET in amyotrophic lateral sclerosis. *Neurology*. 2014;83:1067-74.
17. Marini C, Cistaro A, Campi C, et al. A PET/CT approach to spinal cord metabolism in amyotrophic lateral sclerosis. *Eur J Nucl Med Mol Imaging*. 2016;43:2061-71.

18. Yamashita T, Hatakeyama T, Sato K, et al. Flow-metabolism uncoupling in the cervical spinal cord of ALS patients. *Neurol Sci.* 2017;38:659-665.
19. Marini C, Morbelli S, Cistaro A, et al. Interplay between spinal cord and cerebral cortex metabolism in amyotrophic lateral sclerosis. *Brain.* 2018;141:2272-2279.
20. Brooks BR, Miller RG, Swash M, Munsat TL, World Federation of Neurology Research Group on Motor Neuron Diseases. El Escorial revisited: revised criteria for the diagnosis of amyotrophic lateral sclerosis. *Amyotroph Lateral Scler Other Motor Neuron Disord.* 2000;1:293-9.
21. Rascovsky K, Hodges JR, Knopman D, et al. Sensitivity of revised diagnostic criteria for the behavioural variant of frontotemporal dementia. *Brain.* 2011;134:2456-77.
22. Kimura F, Fujimura C, Ishida S, et al. Progression rate of ALSFRS-R at time of diagnosis predicts survival time in ALS. *Neurology.* 2006;66:265-7.
23. Varrone A, Asenbaum S, Vander Borgh T, et al. EANM procedure guidelines for PET brain imaging using 18F-FDG, version 2. *Eur J Nucl Med Mol Imaging.* 2009;36:2103-10.
24. Borghammer P, Jonsdottir KY, Cumming P, et al. Normalization in PET group comparison studies-the importance of a valid reference region. *Neuroimage.* 2008;40:529-540.
25. Dobson AJ BA. An introduction to generalized linear models, third edition.; 2008.
26. Zimmer ER, Parent MJ, Souza DG, et al. 18F-FDG PET signal is driven by astroglial glutamate transport. *Nat Neurosci.* 2017;20:393-395.
27. Corcia P, Tauber C, Vercoullie J, et al. Molecular imaging of microglial activation in amyotrophic lateral sclerosis. *PLoS One.* 2012;7:e52941.
28. Dupuis L, Pradat P-F, Ludolph AC, Loeffler J-P. Energy metabolism in amyotrophic lateral sclerosis. *Lancet Neurol.* 2011;10:75-82.

**FIGURES:**

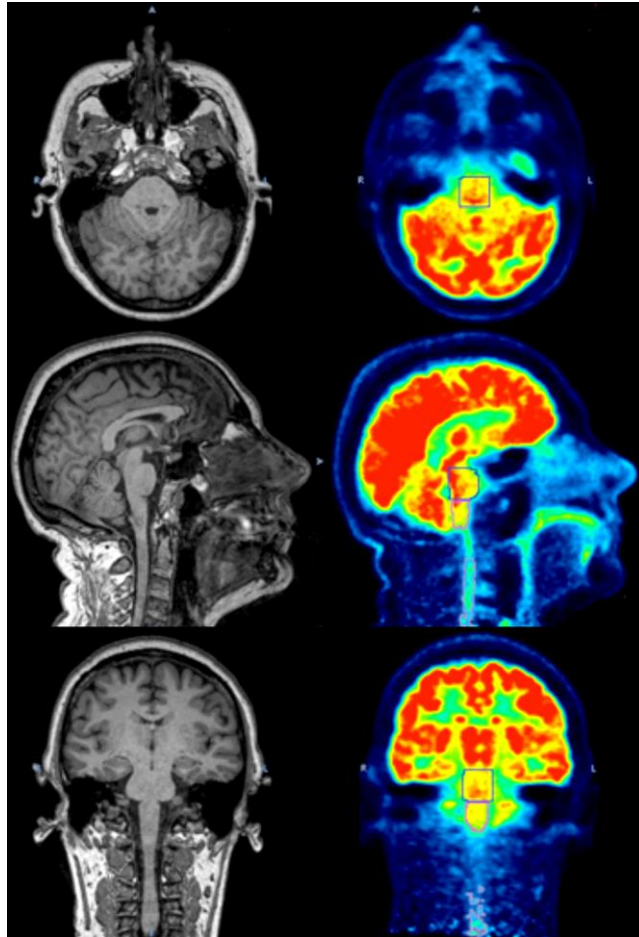


**Figure 1:** MR and PET images: on the right,  $^{18}\text{F}$ -FDG PET images showing the VOIs created using the corresponding T1-weighted MR images. Top, axial; middle, sagittal; bottom, coronal views.

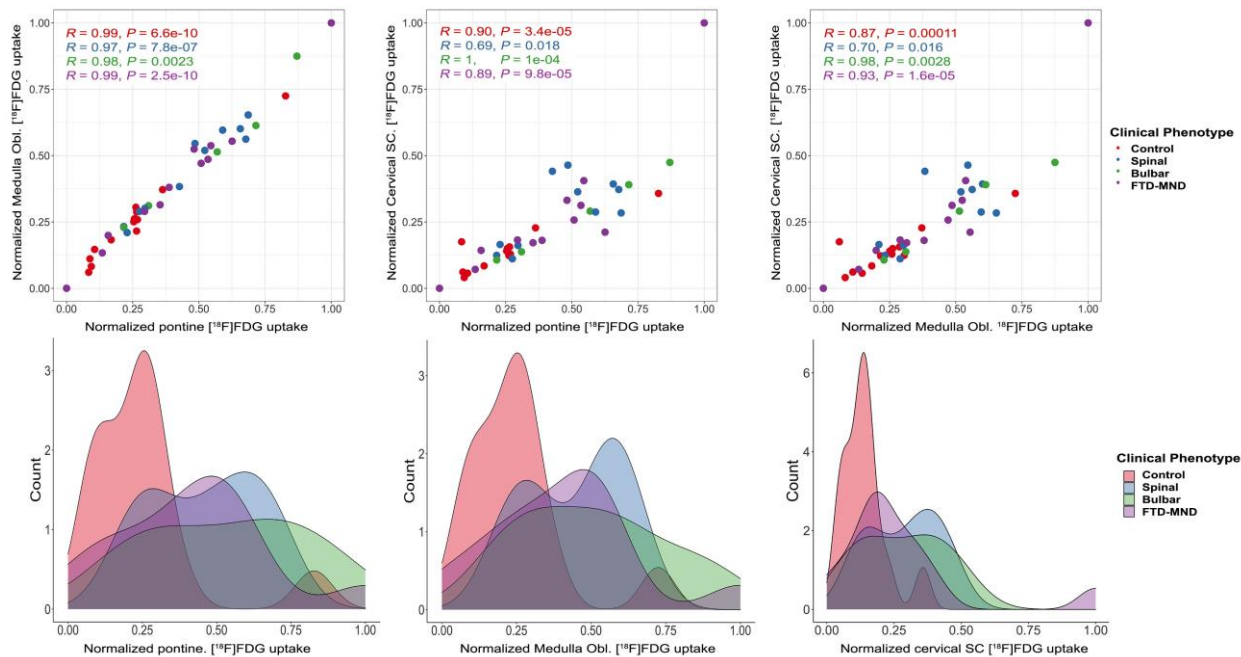


**Figure 2.** First row (A): paired plots showing a strong correlation between the uptake values in the three regions of each subgroup. Red, controls; Blue, Spinal onset; Green, Bulbar onset; Purple, FTD-MND. Second Row (B): density plots displaying the frequency of patients displaying low (such as controls) or high (such as the ALS/FTD continuum) uptake of  $^{18}\text{F}$ -FDG for each subgroup.

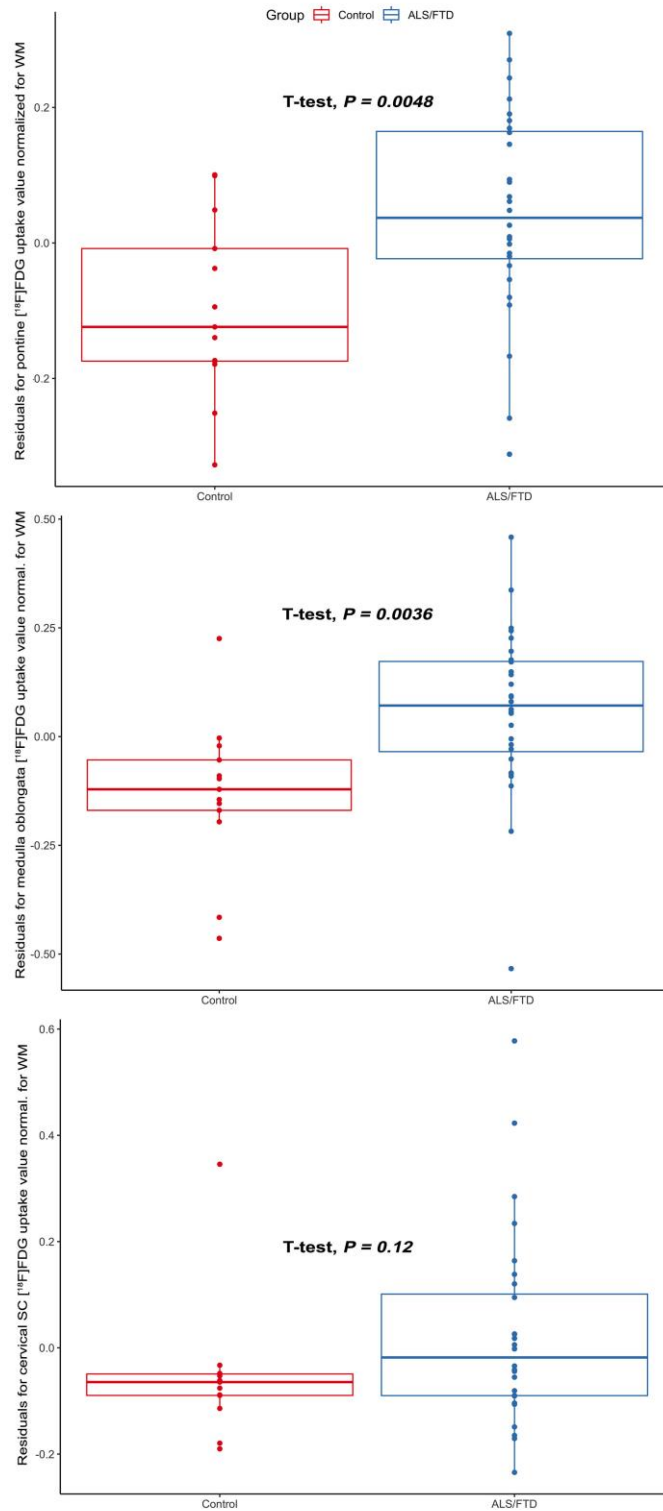


**Figure 3:** Results of the residual analysis for regression between controls and patients (ALS/FTD) normalized uptake values. a. Midbrain/pons. b. Medulla oblongata. c. Cervical spinal cord.

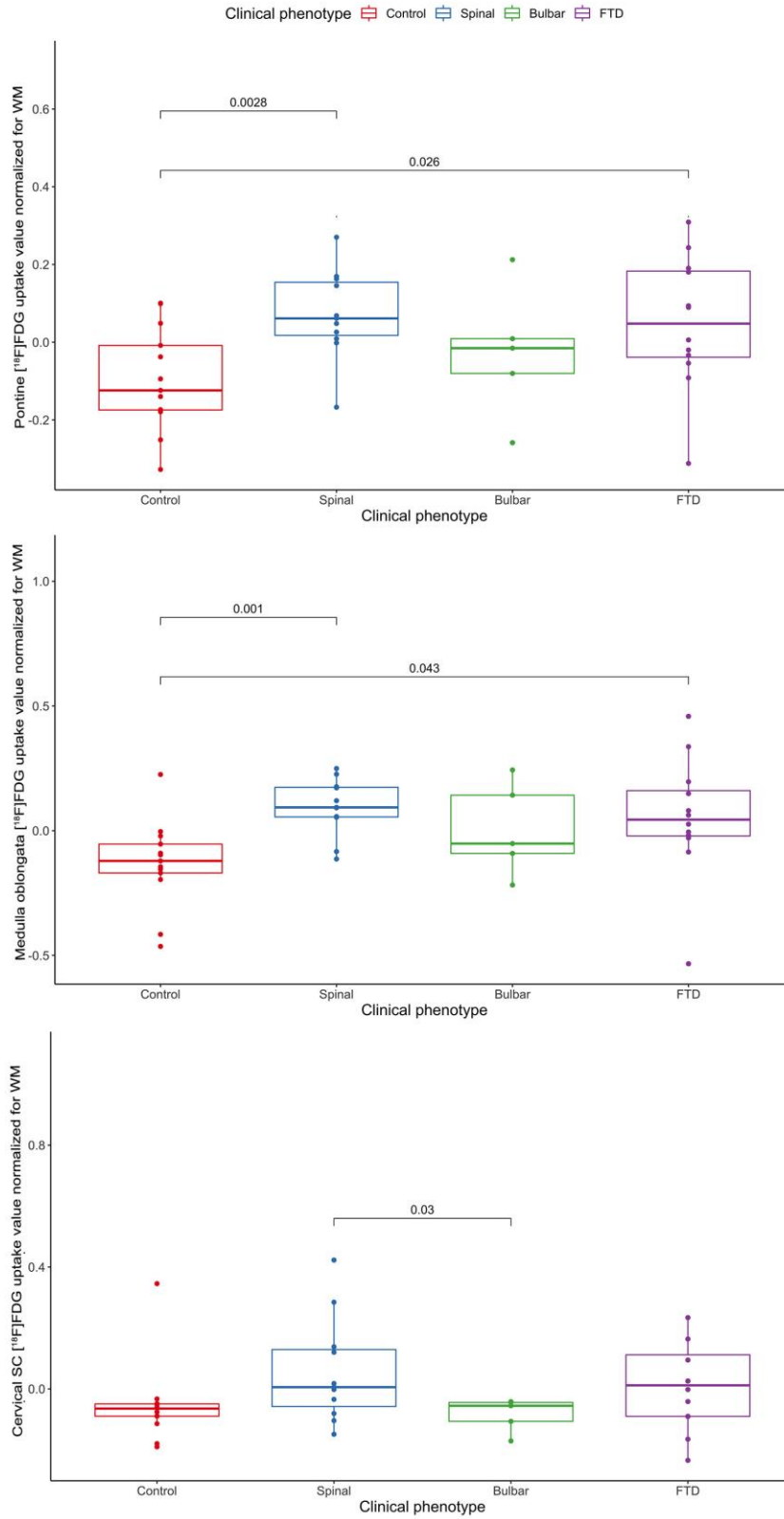


**Figure 4:** Subgroup analysis for <sup>18</sup>F-FDG uptake values.

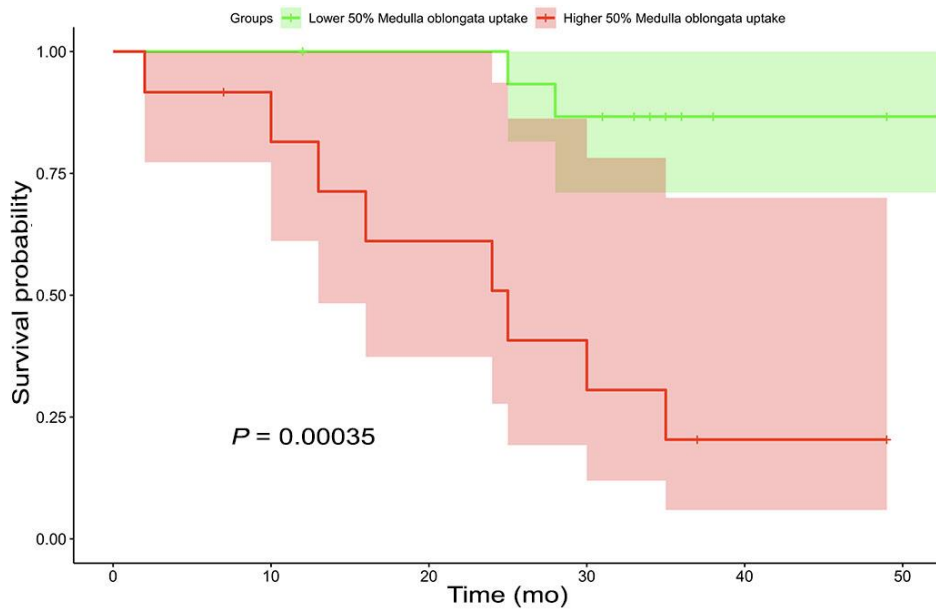


**Figure 5:** Kaplan Meier curve. After the normalization of the uptake values for the occipital white matter, patients were split into two subgroups: the 14 individuals with medulla oblongata uptake over the 50<sup>th</sup> percentile (red) showed a significantly reduced survival than patients with medulla oblongata uptake below the 50<sup>th</sup> percentile (green). Survival expressed in months after the PET-MR scan, p-value calculated through log-rank test

<b>Characteristics</b>	<b>ALS/FTD patients</b>	<b>Controls</b>	<b>P</b>
Sex, M/F	15/13	10/3	0.279
Weight, kg	69.4 +/- 12.1	76 +/- 11.8	0.115
Height, m	1.68 +/- 0.10	1.73 +/- 0.07	0.123
Age at PET, years	62.6 +/- 8.2	52.8 +/- 13.6	0.0035
C9orf72 mutation	6/28	0/13	-
Site of onset:			
Bulbar	5/28		
Spinal	11/28		
Cortical	12/28		

**Table 1:** Clinical and demographic characteristics of the study subjects.

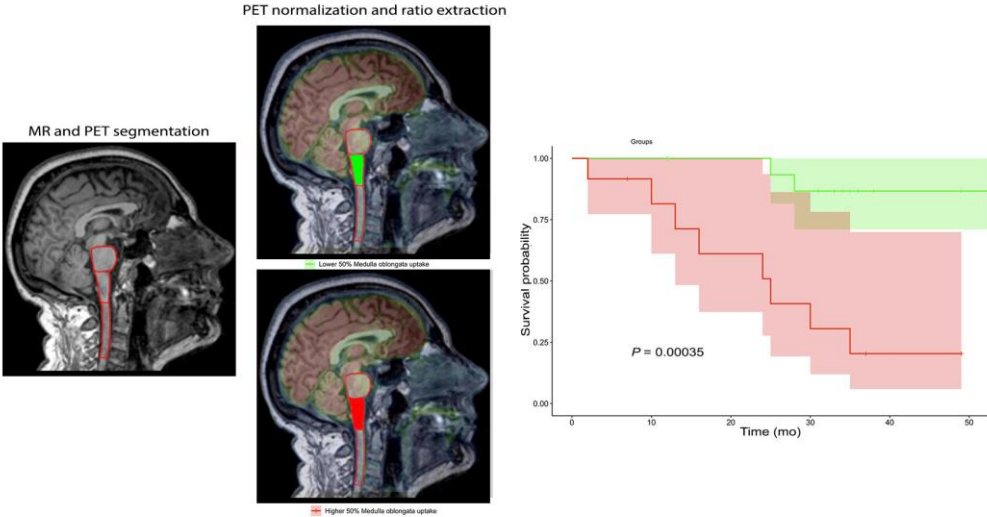
CLINICAL PHENOTYPE	SEX	DEAD	AGE at PET	GENETIC	FIRST ALSfr	LAST ALSfr	PROGRESSION RATE	TIME FROM SYMPTOM ONSET TO PET (months)
Spinal	M	No	55	negative	45	37	0.43	7
Spinal	F	No	60	negative	46	44	0.08	25
Spinal	M	No	55	negative	43	36	0.71	8
Spinal	M	No	63	negative	37	37	0.23	47
Spinal	F	No	54	C9orf72	42	18	0.18	53
Spinal	F	No	67	C9orf72	41	24	0.20	69
Spinal	F	No	76	unknown	32	30	0.67	23
Spinal	F	Yes	58	negative	37	4	0.65	17
Spinal	M	Yes	62	VCP	40	20	0.07	163
Spinal	F	Yes	61	negative	39	33	0.49	21
Spinal	M	Yes	51	negative	40	27	1.33	28
Bulbar	F	No	73	negative	45	24	0.13	24
Bulbar	M	No	68	negative	/	/	/	12
Bulbar	M	No	75	negative	42	36	0.26	30
Bulbar	F	Yes	76	negative	32	23	0.89	18
Bulbar	M	Yes	74	negative	44	44	0.33	13
FTD-UMN	F	No	72	unknown				41
FTD-UMN	M	No	52	C9orf72				20
FTD-UMN	M	No	56	negative				4
FTD-UMN	F	No	55	C9orf72				22
FTD-UMN	F	No	64	C9orf72				28
FTD-UMN	M	No	60	negative				23
FTD-UMN	F	No	63	negative				22
FTD-UMN	M	No	68	negative				17
FTD-UMN	M	Yes	68	unknown				96
FTD-UMN	F	Yes	73	C9orf72				48
FTD-UMN	M	Yes	52	negative				33
FTD-UMN	M	Yes	61	negative				18

**Table 2:** Clinical characteristic at a single subject level

Factor		Univariate Survival Analysis		Multivariate Survival Analysis	
		Hazard ratio (95% Conf Interval)	P Value	Hazard ratio (95% Conf Interval)	P Value
Medulla oblongata uptake		10.2 (2.14-48.56)	<b>0.00352</b>	1.016e+07 (15.95 - 6.47e+12)	<b>0.0180</b>
Age at PET		1.02 (0.93-1.11)	0.642	0.6667 (0.42-1.05)	0.0845
Site of onset	Bulbar	1 (reference)	–	1 (reference)	–
	Spinal	0.8532 (0.15-4.67)	0.855	5.459e-06 (5.23e-11 – 0.57)	<b>0.0398</b>
	FTD	0.8532 (0.15-4.67)	0.855	3.716e-06 (2.6e-11 – 0.53)	<b>0.0390</b>
Genetics	Negative	1 (reference)	–	1 (reference)	–
	VCP	2.4632 (0.29-20.67)	0.406	0.1239 (8.01e-07 -1.923+4)	0.7320
	C9orf72	0.3441 (0.04-2.8)	0.319	1.161e+03 (0.148 – 9.07e+06)	0.1228
	Unknown	1.0770 (0.13 – 8.78)	0.945	5.778e+04 (0.12 – 2.8e+10)	0.1008
Time from onset to PET		1.008 (0.99 – 1.02)	0.233	1.152 (1.02 -1.29)	<b>0.0175</b>

**Table 3:** Univariate and Multivariate Survival analysis. An higher medulla oblongata uptake and a longer time from symptoms onset to PET are associated with a shorter survival. In bold significant results.

**Graphical Abstract:**



**Implications:**  
An increase in glucose metabolism in ALS/FTD patients, as compared to controls, was noted in the three regions under examination (midbrain/pons, medulla oblongata, cervical spinal cord). A multivariate Cox regression analysis confirmed that an higher medulla oblongata uptake is independently associated ( $p:0.0018$ ) with a shorter survival.